Experimental in vivo Imaging of the Cranial Perineural Lymphatic Pathway

John M. Pile-Spellman[1]
Kenneth A. McKusick
H. William Strauss
John Cooney
Juan M. Taveras

After intraventricular injection of ^{99m}Tc antimony sulfide in rabbits (n = 12) and cats (n = 14), radiolabeled colloid was imaged passing into the nasal mucosa and subsequently into the cervical lymph nodes. The cervical lymph nodes accounted for about 12% of the injected dose in rabbits sacrificed at 22–24 hr after injection and about 5% of the injected dose in cats sacrificed at 5–6 hr after injection. In both animals this represented at least one-third of the cerebrospinal fluid colloid clearance. This technique is applicable to in vivo imaging studies of the perineural lymphatic pathway for cerebrospinal fluid absorption in primates and, with modifications, in human subjects.

The perineural lymphatic pathway (PLP) has been demonstrated in a variety of animals using a broad array of imaging agents [1–29]. Materials injected into the cerebrospinal fluid (CSF) can be seen passing along the olfactory nerve into the nasal mucosa and cervical lymphatics. Although the PLP or accessory pathway may be present around all nerves to some extent, the olfactory nerve is the predominant site of CSF efflux by the PLP [1–4].

The PLP carries a significant proportion (at least 15%–30%) of CSF efflux under physiologic conditions (17, 21–24]. The PLP behaves as a bulk-flow drainage pathway. Materials of different molecular weights (60,000–150,000) are cleared at nearly identical rates [21–24). The PLP appears to be pressure-dependent. McComb et al. [30] showed that at higher intracranial pressures, intracisternal dyes and tracers were cleared into the periorbital and nasal tissue at higher rates. The pathophysiology of the PLP is largely unknown, except for its relation to communicating hydrocephalus and central nervous system infections in some animals [31–38].

Evidence for a PLP in primates and humans is conflicting [7, 11, 31, 32, 39–42]. Since researchers have stressed the similarity between primates and cats in CSF absorption dynamics, it is noteworthy that a PLP has been demonstrated in the latter [32, 42]. We report an experimental technique for visualization of the PLP in the intact animal, which has been applied in cats and rabbits. With modifications, this imaging method may be applicable to clinical studies.

Materials and Methods

About 0.20 ml of $^{99m}TcSb_3S_2$ (antimony sulfide) colloid (370 MBq/ml) was instilled into the lateral ventricles of rabbits (n = 12) and cats (n = 14) and viewed with a Nuclear Services, Inc., upgraded HP Pho Gamma III camera with a 3-mm-aperture pinhole collimator, interfaced to a Mod Comp III computer.

Regions of interest for the cranial CSF, olfactory bulb, nasal mucosal region, and cervical lymph nodes were assigned and analyzed. The animals were then sacrificed, and relevant tissues were analyzed for radionuclide activity.

Received June 21, 1983; accepted after revision March 15, 1984.

[1] All authors: Department of Radiology, Massachusetts General Hospital and Harvard Medical School, Boston, MA 02114. Address reprint requests to J. M. Pile-Spellman.

AJNR 5:539–545, September/October 1984
0195–6108/84/0505–0539

Surgical Preparation and Injection Technique

Adult white New Zealand rabbits (weight, 1.8–2.4 kg) and adult cats (weight, 2.0–3.2 kg) were anesthesized with ketamine hydrochloride (0.1 mg/kg for rabbits, 0.1 mg/kg for cats). Using aseptic technique, a 4-cm midline incision was made over the sagittal suture and a ¼-inch (6.4 mm) twist hole made through either the left or the right parietal bone down to—but not through—the dura. In the rabbits, a 23-gauge needle was passed freehand into the lateral ventricle through the hole 7 mm caudal to the coronal suture and 8 mm lateral to the sagittal suture. After slowly injecting the radiolabeled colloid into the ventricles, the needle was removed and the burr hole simultaneously bone-waxed. In the cats, a 23-gauge needle connected to a nanometer filled with 9% saline was stereotaxically lowered to a depth of 15 mm through a burr hole 6 mm caudal to the coronal suture and 2 mm lateral to the sagittal suture. The needle was raised slowly until the saline level dropped, indicating ventricular entry, which typically occurred at a depth of 11–12 mm. The needle was cemented in place and the tracer injected.

Imaging and Biodistribution

The rabbits were imaged at 1-, 3-, or 10-min intervals alternately in standardized anterior or left lateral projections. Eight rabbits were imaged for 8 hr and four rabbits were imaged for 20–24 hr. The cats were maintained in a stereotaxic frame and imaged continuously at 1-min intervals for 4 hr in the anterior projection.

The rabbits were killed with 0.1 ml intravenous euthanasia solution 20–24 hr after injection of tracer; the cats were killed 5 hr after injection of tracer. Their organs were harvested and analyzed using a Packard Auto Gamma System Well Counter against a standard dose (1 ml of a 1/100 dilution of the injected dose).

Image Analysis

All counts were decay-corrected to the time of injection. The total counts from the entire field of view on the initial image for each animal was designated the "total initially viewed counts." This number was considered to represent 100%, and subsequent data were analyzed as percentages of it.

Using a late image, the following anatomic structures were defined and outlined: cranial and upper cervical CSF; nose and olfactory bulb; left and right cervical nodes; and background. Regions of interest did not overlap. Using these described regions, all previous images for that animal were then analyzed.

Results

The biodistribution data in the cat and rabbit and the in vivo digital data in the cat support the visual qualitative impression that the PLP carried a significant portion of CSF efflux in these animals.

Images

Anterior and left lateral images in the rabbit and the cat are presented in figure 1. Dissection of the animals under the gamma scintillation camera confirmed the relations between the images and the anatomy as diagrammed in figure 2.

After intraventricular injection, ^{99}Tc antimony sulfide colloid passed into the basal cisterns and subarachnoid space, then into the nasal mucosa, and finally into the deep cervical lymph nodes (figs. 1 and 2). The olfactory bulb region was visible after 5–10 min and increased in activity over the next 2–3 hr. The upper cervical cord and the fanlike pattern of the nasal mucosa appeared after 10 min. Cervical lymph nodes could be distinguished at 30–40 min after injection and were clearly visible at 1 hr. Cervical lymph node activity increased over the next 1.5–2 hr.

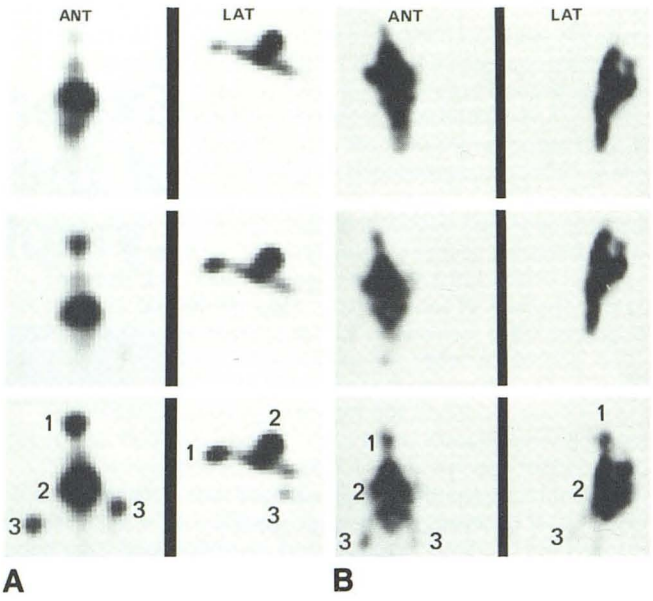

Fig. 1.—Cranial scintigrams. Anterior and left lateral views of rabbit (**A**) and cat (**B**) 0.5, 2, and 4 (**A**) or 6 (**B**) hr (top to bottom, respectively) after intraventricular injection of ^{99m}Tc antimony sulfide colloid. Initially, radiolabeled colloid is confined to cranial CSF (2). After about 10 min, tracer is seen in olfactory bulb–nasal mucosa region (1). From there it passes into deep cervical lymph nodes (3). Cervical lymph nodes are first visible at 40 min after injection and increase markedly in activity over next few hr.

Quantitative in vivo Data

Decay-corrected counts from constant regions of interest are presented as a percentage of the total initially viewed counts (fig. 3). The radiolabeled colloid left the brain-cervical CSF region, falling rapidly to 50% in the first 2 hr in the rabbit and to 45% in the cat. After 2 hr, the brain-cervical CSF activity fell more slowly. The nasal mucosa and olfactory bulb areas in both animals increased to 5% at 1 hr and to 10% over the next 2 hr. The cervical lymph node activity increased to 14% in rabbits and 5% in cats by 3–4 hr. No lymph-node uptake was noted in the cats for the first 30 min.

Biodistribution

Table 1 shows the percentage of injected dose per organ and per gram in rabbits sacrificed at 20–24 hr after injection and in cats sacrificed at 5 hr after injection. Since the choroid plexus concentrated a significant fraction of the dose, our failure in rabbits to separate the choroid from brain before measurement led to an overestimation of total brain-choroid activity.

In the cat the total dose retained in CSF and brain was 20% of the injected dose. The choroid plexus had the highest

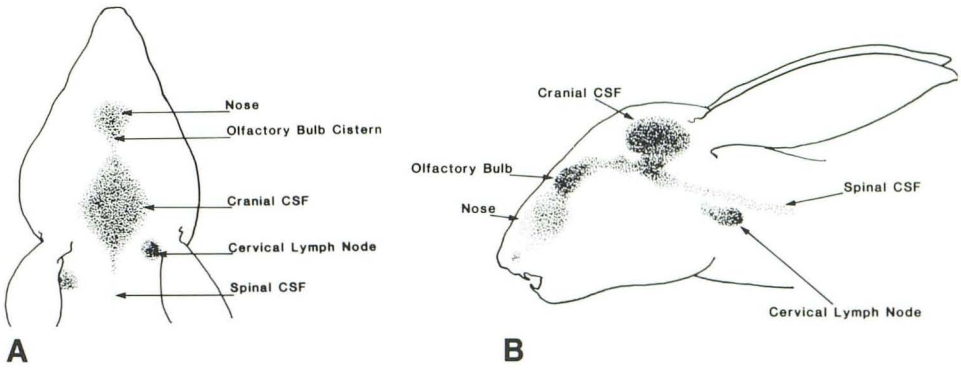

Fig. 2.—Schematic left anterior (**A**) and lateral (**B**) cranial views of rabbit at 4 hr after intraventricular injection of ^{99m}Tc antimony sulfide colloid. *Shaded areas* represent regions of tracer activity.

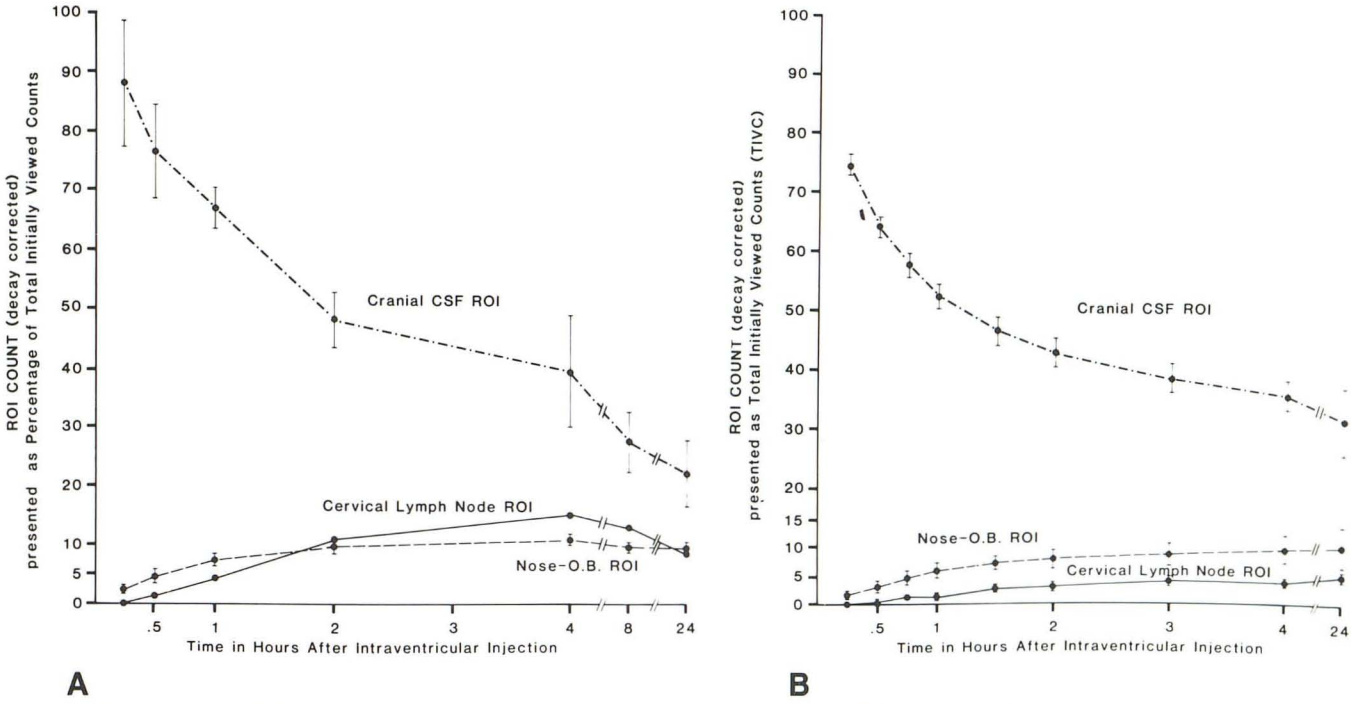

Fig. 3.—Region-of-interest (ROI) data from rabbits (**A**) and cats (**B**) after intraventricular injection of ^{99m}Tc antimony sulfide colloid. Initially, radiolabeled colloid is confined to cranial CSF. After 10–15 min, tracer was seen in olfactory bulb (O.B.) cistern–nasal region; after about 30 min, it was seen in cervical lymph nodes. Activity in cervical lymph nodes increased to 14% of total initially viewed counts in rabbits and 5% in cats.

concentration per gram of any tissue. The cervical lymph node activity at about 15% of injected dose was 400 times higher than in the mesenteric nodes. In the rabbit the cervical lymph node activity at about 75% of dose per gram also was markedly greater than mesenteric lymph node activity, which was 0.16% (injected dose/g).

Discussion

The PLP was thought to be the predominant drainage route of CSF in 1869, when Schwalbe [5] demonstrated that Berlin blue dye, when injected into the canine subarachnoid space, collected in the cervical lymphatics. That concept persisted until 1914, when Weed [1] injected a solution of ferrous cyanide into the lateral ventricles of rabbits and cats. He then perfused the animals with acid, causing the crystals to precipitate by acid fixation. He found the blue crystals primarily in the arachnoid villi and venous sinuses. Although some of the crystals were found along the cranial nerves and cervical lymphatics, Weed emphasized that the major pathway for CSF efflux was the arachnoid villi–venous pathway [1].

The PLP was progressively disregarded until recent work by Bradbury and others rekindled interest [18, 21–24]. Their work, based on observations made some 25 years earlier, showed that tracers injected into the subarachnoid space could be recovered from the cervical lymphatics by cannulation of the main jugular lymphatic duct [17]. Bradbury et al. [18] demonstrated that the PLP was important in its absolute and relative contribution to CSF absorption. The cranial PLP's absolute contribution to CSF absorption varied among species studied, with 14%–30% of the injected dose begin recovered from the cervical lymphatics (in the rabbit, 30%). The

TABLE 1: **Biodistribution of ^{99m}Tc Antimony Sulfide Colloid afer Intraventricular Injection in Rabbits and Cats**

Animal: Organ or Site (*n*)	% of Dose (Mean ± SD)	
	/Organ	/g
Rabbit:		
Brain and choroid plexus (6)	...	11.66 ± 19.87
Cerebrospinal fluid (4)	7.87 ± 5.92	3.44 ± 2.67
Nose (4)	...	12.33 ± 19.97
Cervical lymph nodes (6)	11.71 ± 9.76	77.65 ± 59.97
Liver (6)	20.19 ± 17.30	0.20 ± 0.20
Spleen (6)	0.34 ± 0.56	0.22 ± 0.36
Kidneys (6)	16.02 ± 20.56	0.67 ± 0.81
Injection site (4)	...	0.21 ± 0.29
Abdominal lymph nodes (4)	0.04 ± 0.04	0.16 ± 0.16
Blood (6)	2.85 ± 3.14	1.06 ± 2.42
Urine (6)	...	0.81 ± 1.00
Cat:		
Brain (10)	16.36 ± 9.22	0.63 ± 0.38
Cerebrospinal fluid (10)	2.91 ± 1.46	0.58 ± 0.29
Choroid plexus (9)	...	24.83 ± 18.37
Dura mater (7)	...	1.27 ± 1.02
Nose (9)	...	0.91 ± 0.58
Cervical lymph nodes (10)	4.71 ± 3.57	4.84 ± 4.46
Liver (10)	9.58 ± 2.37	0.11 ± 0.05
Spleen (8)	0.39 ± 0.21	0.04 ± 0.02
Kidneys (9)	3.63 ± 0.98	0.14 ± 0.06
Injection site (7)	<0.005	0.21 ± 0.52
Mesenteric lymph nodes (6)	<0.005	0.01 ± 0.01
Sudmandibular gland (5)	0.04 ± 0.04	0.19 ± 0.35
Eye (9)	0.05 ± 0.08	0.01 ± 0.01
Blood (10)	4.95 ± 1.90	0.02 ± 0.01
Urine (8)	...	0.17 ± 0.09

Note.—Rabbits were sacrificed for tissue analysis at 20–24 hr after injection; cats were sacrificed at 5 hr after injection.

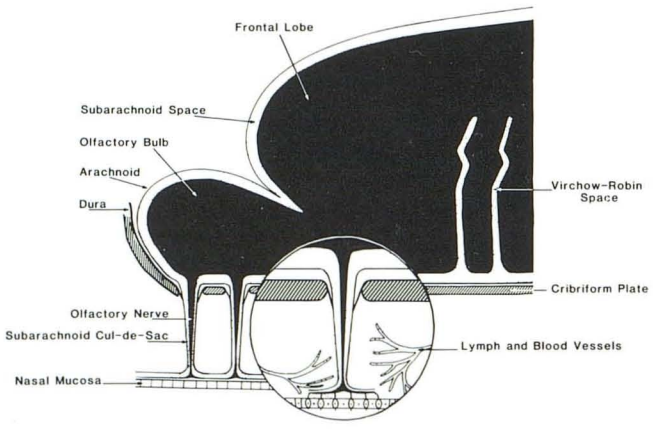

Fig. 4.—Diagram of olfactory nerve portion of perineural lymphatic pathway in rabbits and cats (adapted from [3] and [18]). Radiolabeled tracer (represented by *dots*) is seen in subarachnoid space. It flows freely out the cranial vault into subarachnoid cul-de-sac, then passes through perineurium to interstitial space of nasal mucosa. From here, the smaller-sized particles may pass into blood vessels or lymph channels. Larger molecules (10–120 nm diam) can be cleared only by the lymphatic channels and tend to be trapped in lymph nodes downstream.

relative contribution of the cranial PLP to CSF absorption was calculated to be 40%; that is, an estimated 40% of the CSF absorption in the rabbit takes place via the PLP.

After intraventricular injection of a radiolabeled colloid, we found that 12% of the total injected dose was retained by the cervical lymph nodes in rabbits and 5% in cats. This does not represent total clearance via the PLP, since it does not include that portion of the radiolabeled colloid which passed through the lymph nodes to enter the central venous circulation. Indeed, both our results and those results predicated upon cannulation of the cervical lymph duct underestimate the absolute contribution of the PLP to CSF clearance. First, the results do not include the known clearance along dorsal spinal roots. Second, the results do not include the nonlymphatic capillary–venous clearance from the nasal interstitium.

From our results it is possible to estimate that the contribution of the PLP to total CSF colloid clearance was at least 33%. This estimate can be calculated by assuming that (1) the cervical lymph node activity accounts for all PLP activity, (2) the cervical lymph node activity is not contaminated by nonspecific recirculation of activity from the blood pool or leakage from the injection site, (3) all liver activity is from the arachnoid villi–venous pathway, and (4) the extraction of the tracer by the liver and lymph node is similar [43–46]. These assumptions will underestimate the contribution of the PLP to CSF clearance or overestimate the contribution of the arachnoid villi–venous pathway to CSF colloid clearance. The cervical node activity indicates PLP colloid clearance, and the liver activity indicates arachnoid villi–venous pathway colloid clearance. The ratio of cervical node activity to liver activity in both the rabbit and the cat in our study was about 1:2,

indicating that at least 33% of the CSF clearance was via the PLP.

Imaging and analysis of the PLP is possible because of the properties of ^{99m}Tc antimony sulfide, an inert radiolabeled colloid containing particles 10–120 nm in diameter. It is used clinically for lymphoscintigraphy [43–46]. The size of the particles in a material largely determines its clearance from an interstitial space [46]. Particles less than 10 nm in diameter pass readily through the fenestrated basement membranes of blood-vessel capillaries. Materials containing particles larger than 10 nm in diameter are cleared by the lymphatics, either by bulk flow or by pinocytosis into the lymph channel. After subcutaneous injection of ^{99m}Tc antimony sulfide in the rabbit, 80% of the injected dose remains at the injection site at 4 hr, 2% of the dose can be recovered from the regional lymph nodes, and most of the remainder is in the reticuloendothelial system of the liver [47]. Intravascular clearance of the radiolabeled colloid is mainly via the latter system, with 75% of the injected dose in the liver at 2 hr after injection [47].

Previous attempts to image the PLP have been successful in rabbits and dogs, but have failed repeatedly in cats and primates [32, 42]. Images of the cranial PLP have been obtained in both the rabbit and dog using either Thorotrast (thorium dioxide) or iodinated oils (Brominol or Pantopaque) [11, 12, 15, 32, 42]. Stuck and Reeves [42], using intraventricular injections of Thorotrast in cats and monkeys, opacified the optic nerve sheath but could not detect any extracranial Thorotrast in excrement or in the sacrificed animals' ashes. From similar experiments using Thorotrast and Pantopaque [32], Schurr et al. [31] also concluded that the PLP was an important pathway in dogs but insignificant or absent in cats and primates. Why the PLP could not be visualized using Thorotrast in cats is not known. The rate of CSF clearance of colloid by all routes is slower in the cat than in the rabbit. It has been shown that in animals followed for up to 6 months, no additional Thorotrast movement occurs 8 hr after injection [15]. Slower clearance of colloid with subsequent binding may account for the inability to visualize the PLP with Thorotrast in cats.

It was possible to image the PLP in both cats and rabbits after intraventricular injection of ^{99m}Tc antimony sulfide. The radiolabeled colloid passed into the basal cisterns and (within 5 min) to the area of the olfactory bulb–cribriform plate, then into the nose. Cervical lymph node activity was first seen after 30 min. Activity in the nose–olfactory bulb region reached 90% of maximum at about 2 hr in the rabbit and 3 hr in the cat. The cervical lymph node region reached 90% of maximum at about 2 hr in the rabbit and 3 hr in the cat. The cranial-CSF activity fell to 50% of its initial activity at 2 hr in both animals.

The images (fig. 1) show that the olfactory bulb–cribriform plate area is the predominant site of cranial CSF colloid clearance. Obliteration of the olfactory nerve and cribriform plate by surgical ablation and replacement with methylmethacrylate has been shown to cause a 90% decrease in the amount of tracer recovered by cervical lymphatic duct cannulation [24]. Surgical ablation destroys not only the olfactory nerves, but the subarachnoid sheath that extends along the nerves for some distance extracranially. This area is termed the "subarachnoid cul-de-sac." How material gets from the subarachnoid cul-de-sac into the nasal interstitial space is not known; it must, however, pass through the layers of cells that are covering the extracranial portion of the olfactory nerve. A schematic drawing of the subarachnoid cul-de-sac and the surrounding tissue is shown in figure 4.

Once the olfactory nerves pierce the cribriform plate, their dura and arachnoid fuse and approximate the pia of the nerve and become continuous with the epineurium [48]. Materials injected into the CSF can be recovered from both the subarachnoid space and the "subepineurial" space [48]. Beneath the epineurium, the perineurium covers the individual nerve fasciculi and is continuous with the subarachnoid-pia. The perineurium acts as both a barrier and a bridge [48], protecting the nerve from viral infections and providing a site for active transport.

The PLP has not been demonstrated convincingly in man. Key and Retzius [7], using gelatin injection in cadavers, demonstrated a connection between the olfactory subarachnoid space and the cervical lymph nodes. This connection was thought by some to be an artifact produced by the long, high-pressure injections (60–80 cm Hg) [1]. Jacobi and Lohr [40], collaborators of Egar Moniz, reported visualization of the PLP in human subjects with subarachnoid injections of Thorotrast. Although their description of the PLP with Thorotrast is similar to findings in dogs and rabbits, no radiographs or pertinent subject data were provided. Opacification of the PLP by Thorotrast has not been reported by other researchers [49]. Computed tomography (CT) performed after intrathecal injection of metrizamide in human subjects has demonstrated contrast material along the arachnoid cul-de-sac of the optic nerve sheath. If metrizamide did opacify the tiny olfactory nerve root cul-de-sacs, it would be very difficult to see because of the problems of partial-volume effect and resolution with CT. With a molecular weight (MW) of 789, metrizamide would not be trapped in the cervical lymph nodes. Neither would routine clinical radionuclide cisternography be expected to demonstrate a PLP in man. The agents commonly used are small (radioiodinated serum albumin, MW 60,000; pentetate [DTPA], MW 398), and if they were to leave the CSF via the PLP, they would not become trapped in cervical lymph nodes but would be quickly cleared by the venous capillary bed of the nose.

Occult CSF rhinorrhea is diagnosed routinely with ^{111}In DTPA cisternography [50]. Even in patients without CSF rhinorrhea, after cisternography there is significant activity in nasal secretions that is similar to the peak blood concentrations [51]. This activity has been presumed to be from active concentration and secretion of the tracer by the nasal mucosa from the tracer in the blood pool. DiChiro et al. [34] using radioiodinated human serum albumin cisternography in dogs, showed that the marked nasal activity seen in dogs could not have come from the blood pool but was related to CSF clearance.

If a significant PLP is not present in man, the use of an animal with a significant PLP for experimental modeling of

such diseases as hydrocephalus would have to be seriously questioned. Cats are now considered by many to be an adequate model for hydrocephalus [32]. Our data indicate that in cats the PLP may account for at least one-third of CSF clearance.

Demonstration of an active PLP in man would have implications in cerebral pathophysiology. Foldi and Csillik [25] reported increased intracranial pressure, brain edema, and various histochemical and behavioral changes after removal of all identifiable cervical lymph vessels and nodes in a variety of animals. This has been called "experimental lymphogenic encephalopathy." There is an increase in the efflux via the PLP after experimentally induced increased intracranial pressure, as shown by McComb et al. [30] using a steady-state system in rabbits. If there is an active PLP in man, the popular notion that the brain is an immunologically privileged area should be questioned. Viral agents and amebic infections are known to travel in a retrograde fashion via the PLP of the nose [34–38]. Some viral encephalopathies in man are suspected of entering via the nasal mucosa [36]. It has been shown that sclerosis of the nasal mucosa of mice protects the animals from subsequent nasal viral innoculations [35].

An inert colloid such as ^{99m}Tc antimony sulfide may not be appropriate for use in humans. Inert colloids such as Thorotrast and kaolin have been shown to cause communicating hydrocephalus and an inflammatory arachnoiditis [42]. A biodegradable compound with size properties similar to ^{99m}Tc antimony sulfide, such as microaggregated albumin, however, may be suitable, with appropriate magnetic resonance radionuclide markers.

REFERENCES

1. Weed LH. Studies on cerebrospinal fluid. *J Med Res* **1914**;31:21–117
2. Galkin WS. Zur Methodik der Injektion des Lymph Systems von Subarachnoidalraum aus (Bedeutung der Injektionstelle). *Z Gesamte Exp Med* **1930**;74:182–480
3. Brierley JB, Field EJ. The connexions of the spinal subarachnoid space with the lymphatic system. *J Anat* **1948**;82:153–166
4. Bowsher D. Pathways of absorption of protein from the cerebrospinal fluid: an autoradiographic study in the cat. *Anat Rec* **1957**;128:23–39
5. Schwalbe G. Der Arachnoidalraum: ein Lymphraum und sein Zusammenhang mit den Perichoriodalraum. *Zentralbl Med Wissenschaften* **1869**;7:465–467
6. Quincke H. Zur Physiologic der Cerebrospinalflussigkeit. *Reicherts Arch Anat Physiol* **1872**:153–177
7. Key EAH, Retzius MG. Studien in der Anatomie des Nervensystems und des Bindegewebes. Stockholm: Samson and Wallin, **1875**
8. Flatau TS. Ueber den Zusammenhang der nasalen Lymphbahnen mit dem Subarachnoidealraum. *Dtsch Med Wochenschr* **1890**;16:972–973
9. Dandy WE, Blackfan KD. An experimental and clinical study of internal hydrocephalus. *JAMA* **1913**;61:2216–2217
10. Ivanow G, Romodanowsky K. Über den anatomischen Zusammenhang der cerebralen und spinalen submeningealen Raume mit den Lymphsystem. *Z Gesamte Exp Med* **1928**;58:596–607
11. Wustmann O. Experimentelle Untersuchungen über die Reliefdarsellung (Umrisszeichnung) des Zentral-nervensystems im Röntgenbild durch Thorium-Kontrastmittel. *Dtsch Z Chir* **1933**;238:529–567
12. Mortensen OA, Sullivan WE. The cerebrospinal fluid and the cervical lymph nodes. *Anat Rec* **1933**;56:359–363
13. Tschudnosovetof VA. The influence of types of breathing on the injection of mucosa of the nose after subarachnoid introduction of China ink. *Acta Otolaryngol* (Stockh) **1934**;21:199–218
14. Nelsen EC. *A study of the paths taken by injected materials through the cribriform plate* [Dissertation]. Madison, WI: University of Wisconsin, **1936**
15. Faber WM. The nasal mucosa and the subarachnoid space. *Am J Anat* **1937**;62:121–148
16. Field EJ, Brierley JB. The retro-orbital tissues as a site of outflow of cerebrospinal fluid. *Proc R Soc Lond [Biol]* **1949**;42:447–450
17. Courtice FC, Simmonds WJ. The removal of protein from the subarachnoid space. *Aust J Exp Biol Med Sci* **1951**;29:255–263
18. Bradbury MWB, HF Cserr, Westrop RJ. Drainage of cerebral interstitial fluid into deep cervical lymph of the rabbit. *Am J Physiol* **1981**;240:329–336
19. Orosz A, Foldes I, Kosa C, et al. Radioactive isotope studies of the connection between the lymph circulation of the nasal mucosa, the cranial cavity and cerebrospinal fluid. *Acta Physiol Acad Sci Hung* **1957**;11:75–81
20. Yoffey JM. Passage of fluid and other substances through the nasal mucosa. *J Laryngol Otol* **1958**;72:377–383
21. Bradbury MWB. Proportion of cerebrospinal fluid draining into jugular lymphatic trunks of the cat. *J Physiol* **1977**;276:67–68
22. Bradbury MWB. Cook CCH, Hopkins R. Role of the cervical system in drainage of cerebrospinal fluid. *J Physiol* (Lond) **1977**;266:26P
23. Bradbury MWB. Proportion of cerebrospinal fluid draining into jugular lymphatic trunks of the cat. *J Physiol* (Lond) **1978**;267:67P–68P
24. Bradbury MWB, Cole DF. The role of the lymphatic system in drainage of cerebrospinal fluid and aqueous humour. *J Physiol* (Lond) **1980**;299:353–365
25. Foldi M, Csillik B, Zoltan OT. Lymphatic drainage of the brain. *Experientia* **1968**;24:1283–1287
26. Arnold W, Nitze HR, Ritter R, et al. Qualitative Untersuchungen der Verbindswege des Subarachnoidalraumes mit dem lymphatischen System des kopfes und des Halses. *Acta Otolaryngol* (Stockh) **1972**;74:411–424
27. Arnold W, Ritter R, Wagner WH. Quantitative studies on the drainage of the cerebrospinal fluid into the lymphatic system. *Acta Otolaryngol* (Stockh) **1973**;76:156–161
28. Casley-Smith JR, Foldi-Borcsok E, Foldi M. The prelymphatic pathways of the brain as revealed by cervical lymphatic obstruction and the passage of particles. *Br J Exp Pathol* **1976**;57:179–188
29. Duckert LG, Duvall AJ. Cochlear communication routes—spiral ganglia and osseous spiral laminae. *Otolaryngology* **1978**; 86:434–446
30. McComb JG, Davidson H, Hyman S, Weiss MH. Cerebral fluid drainage as influenced by ventricular pressure in the rabbit. *J Neurosurg* **1982**;560:790–797
31. Somberg HM. The relation of the spinal subarachnoid and perineural spaces. *J Neuropathol Exp Neurol* **1947**;6:166–171
32. Schurr PH, McLaurin RL, Ingraham FD. Experimental studies on the circulation of cerebrospinal fluid, and methods of producing communicating hydrocephalus in the dog. *J Neurosurg* **1953**;10:515–525

33. Cammermyer J. Frequency of meningoencephalitis and hydrocephalus in dogs. *J Neuropathol Exp Neurol* **1961**;20:386–398
34. DiChiro G, Stein SC, Harrington T. Spontaneous cerebrospinal fluid rhinorrhea in normal dogs. Radioisotope studies of an alternative pathway of CSF drainage. *J Neuropathol Exp Neurol* **1972**;31:447–453
35. Clark WELG. *Anatomical investigation into the routes by which infections may pass from the nasal cavities into the brain*. Health Medical Subjects, no. 54. London: Republic, **1929**
36. Johnson RT, Mims CA. Pathogenesis of viral infections of the nervous sytem. *N Engl J Med* **1968**;278:23–30, 84–92
37. Constantine DG, Emmons RW, Woodie JD. Rabies virus in nasal mucosa of naturally infected bats. *Science* **1972**;175:1255–1256
38. Onodera T, Fujiwara K. Nasoencephalopathy in suckling mice inoculated with the Tyzzer's organism. *Jpn J Exp Med* **1973**;43:509–522
39. Zwillinger H. Lymphbahnen des oberen Nasalschuittes und deren Beziehungen zu den perimeningealen Lymphraumen. *Arch Laryngol Rhinol* **1912**;26:66–78
40. Jacobi W, Lohr W. Eine neue Methode zur Reliefdarstellung des zentral Nervensystems in röntgenbild. *Dtsche Z Nervenheilkunde* **1933**;130:15–22
41. Alexander LT, Jung TS, Lyman RS. Colloidal thorium dioxide: its use in intra-cranial diagnosis and its fate on direct injection into the brain and the ventricles. *Arch Neurol Psychiatry* **1934**;32:1143–1158
42. Stuck RM, Reeves DL. Dangerous effects of Thoratrast used intracranially. *Arch Neurol Psychiatry* **1938**;40:86–115
43. Hawkins LA, McAlister JM. The use of ^{99m}Tc antimony sulfide colloid for liver scanning, its preparation and some clinical and experimental observations. *Br J Radiol* **1969**;42:657–661
44. Nagai K, Itoko Y, Otsuka N, et al. Experimental studies on accretion of ^{99m}Tc antimony sulfide colloid in the RES. *Jpn J Nucl Med* **1978**;17:583–587
45. Martindale AA, Papadimitria JM, Turner JH. Technetium-99m antimony colloid for bone marrow imaging. *J Nucl Med* **1980**;21:1035–1041
46. Molinski VJ, Thornton AK. *Biological distribution study after intramuscular administration of* $^{99m}TcSb_2DS_3$, pt 2B. Tuxedo, NY: Union Carbide, **1980**
47. Borguuist L, Strand SE, Persson BRR. Particle sizing and biokinetics of lymphoscintigraphic agents. *Semin Nucl Med* **1983**;13:9–19
48. Jackson RT, Tigges J, Arnold W. Subarachnoid space of the CNS, nasal mucosa and lymphatic system. *Arch Otolaryngol* **1979**;105:180–184
49. Freeman W, Schoenfield HH, Moore C. Ventriculography with colloidal thorium dioxide. *JAMA* **1936**;106:96–101
50. McKusick KA. The diagnosis of traumatic CSF rhinorrhea. *J Nucl Med* **1977**;18:1234–1235
51. McKusick KA, Malmud LS, Kordela P, Wagner HN Jr. Radionuclide cisternography: normal values for nasal secretion of intrathecally injected indium-111 DPTA. *J Nucl Med* **1973**;14:933–934